fluoroacetone, with its unsaturated carbonyl group, can form stronger metal-surface bonds, which suggests that some of the molecules bond in an η^2-geometry. Fluorination *decreases* the chemisorption bond strength of the η^1-molecules by about 12 kJ/mol and *increases* that of the η^2-species by about 20 kJ/mol.

Acknowledgment. We thank R. J. Angelici and T. Upton for valuable discussions. This research has been supported by the Director for Energy Research, Office of Basic Energy Sciences. Ames Laboratory is operated for the U.S. Department of Energy by Iowa State University under Contract No. W-7405-ENG-82.

An Inelastic Electron-Tunneling Spectroscopic Investigation of the Reaction of Molybdenum Oxychlorides with a Hydroxylated Aluminum Oxide Surface

G. J. Gajda, R. H. Grubbs, and W. H. Weinberg*

Contribution from the Division of Chemistry and Chemical Engineering, California Institute of Technology, Pasadena, California 91125. *Received January 26, 1987*

Abstract: Molybdenum oxytetrachloride adsorbs on alumina at 22 °C and reacts with the surface hydroxyl groups to form a dimeric oxydichloride–molybdenum complex. This complex desorbs slowly from the surface, as molybdenum dioxodichloride. Heating the surface during oxytetrachloride exposure yields poorly characterized decomposition products and tunnel junctions with very large conductivity changes as a function of bias voltage. Molybdenum dioxodichloride adsorbs on alumina at 22 °C and forms an oligomerized molybdenum trioxide species. This oxide adsorbs water at a background pressure of approximately 1×10^{-7} Torr, and it can be dehydrated by heating under vacuum to 100 °C. Heating the surface during the vapor-phase exposure of molybdenum dioxodichloride, or the molybdenum oxide under vacuum after the exposure, increases the extent of polymerization. Exposure of the oxide to 2 Torr of ethylene at 100 °C or 10^{-1} Torr of acetic acid at 22 °C produces changes in the tunneling spectra, due to increased oligomerization and some decomposition of the adsorbates, but there is no evidence for molecular adsorption or hydrocarbon formation. Exposure of the oxide to 5×10^{-2} Torr of 4-*tert*-butylpyridine at 22 °C causes the complete desorption of the oxide, presumably as the tripyridine complex.

I. Introduction

Inelastic electron-tunneling spectroscopy is a moderate-resolution (full-width at half-maximum below 20 cm^{-1}), high-sensitivity (fractional surface coverages on the order of 10^{-2} monolayer) technique for measuring the vibrational spectra of molecules adsorbed on insulating surfaces. The theory and practice of inelastic electron tunneling have been reviewed extensively,[1-11] as has the more general class of tunneling spectroscopies.[12] The basic requirement of the technique is the formation of a tunnel junction consisting of two conductors separated by a thin insulating barrier. The surface of this insulator is the one upon which adsorption and reaction occurs.

Although many substrates have been used [e.g., Cr,[13] Y,[13] Ho,[14] Er,[14] Al,[15] and Mg[15]], the insulator in most cases has been the metal oxide formed by oxidation in air or a glow discharge. The majority of tunneling spectra have been obtained on the surfaces of Al_2O_3 and MgO.[15] This restriction has led to an investigation of non-oxide insulators and alternative junction geometries (involving movable electrodes) in a search to broaden the range of applications accessible to tunneling spectroscopy.

Non-oxide barriers have been synthesized primarily by employing reagents other than oxygen in the glow discharge treatment of the metal-film electrode. For example, by using CF_4, a barrier similar to AlF_3 is formed,[16] while using $SO_2 + O_2$ produces an AlS_xO_y barrier similar to aluminum disulfate.[17] A second approach has been the evaporation of low-volatile oxides [e.g., SiO[18]] onto the metal substrate. Variations in the junction geometries are represented by the "squeezable" electron-tunnel junctions.[19] In this technique, two separate metal-film electrodes are fabricated and mechanically positioned crosswise, similar to a standard junction geometry but with an air-gap between them. The supported films are then squeezed together by an electromagnet to reduce the gap between the electrodes to approximately 10–20 Å, necessary for electron tunneling to occur. Although no vibrationally inelastic tunneling spectra have yet been reported by this technique, experiments continue.[19] Similarly, theoretical work has appeared, suggesting the measurement of inelastic spectra via scanning tunneling microscopy.[20]

Molybdenum oxide is used widely as a catalyst for oxidation reactions either by itself or in the form of a mixed oxide.[21] We have observed the formation of molybdenum suboxides by decomposition of molybdenum hexacarbonyl on alumina surfaces,[22] but these suboxides were not suitable insulators for tunneling spectroscopy. We have observed also that metal chloride complexes [e.g., $[Rh(CO)_2Cl]_2$[23]] will react with the hydroxylated

(1) Hansma, P. K. *Phys. Rep. C* **1977**, *30*, 146.
(2) Weinberg, W. H. *Annu. Rev. Phys. Chem.* **1978**, *29*, 115.
(3) *Inelastic Electron Tunneling Spectroscopy*; Wolfram, T., Ed.; Springer: Berlin, 1978.
(4) Hansma, P. K.; Kirtley, J. R. *Acc. Chem. Res.* **1978**, *71*, 440.
(5) White, H. W.; Wolfram, T. *Methods Exp. Phys. A* **1980**, *16*, 149.
(6) White, H. W.; Godwin, L. M.; Elliatioglu, R. *J. Adhes.* **1981**, *13*, 177.
(7) Ewert, S. *Appl. Phys. A* **1981**, *26*, 63.
(8) *Tunneling Spectroscopy*; Hansma, P. K., Ed.; Pleunum: New York, 1982.
(9) Weinberg, W. H. *Vib. Spectra Struct.* **1982**, *11*, 1.
(10) Khanna, S. K.; Lambe, J. *Science* **1983**, *220*, 1345.
(11) *Principles of Electron Tunneling Spectroscopy*; Wolf, E. L., Ed.; Oxford: New York, 1985.
(12) Walmsley, D. G.; Tomlin, J. L. *Prog. Surf. Sci.* **1985**, *18*, 247.
(13) Jaklevic, R. C.; Lambe, J. *Phys. Rev. B* **1970**, *2*, 808.
(14) Adane, A. *Solid State Commun.* **1975**, *16*, 1071.
(15) See, for example, the spectra in ref 12.
(16) Gauthier, S.; De Cheveigne, S.; Salace, G.; Klein, J.; Belin, M. *Surf. Sci.* **1985**, *155*, 31.
(17) Suzuki, M.; Mazur, U.; Hipps, K. *Surf. Sci.* **1985**, *161*, 156.
(18) Mazur, U.; Hipps, K. *J. Phys. Chem.* **1981**, *85*, 2244.
(19) Moreland, J.; Alexander, S.; Cox, M.; Sonnenfeld, R.; Hansma, P. K. *Appl. Phys. Lett.* **1983**, *43*, 387.
(20) Binnig, G.; Garcia, N.; Rohrer, H. *Phys. Rev. B* **1985**, *32*, 1336.
(21) See, for example: *Fourth International Conference: The Chemistry and Uses of Molybdenum*; Climax: Ann Arbor, 1982.
(22) Gajda, G. J.; Grubbs, R. H.; Weinberg, W. H. *J. Am. Chem. Soc.* **1987**, *109*, 66.

0002-7863/87/1509-5627$01.50/0

aluminum oxide surface present in our tunnel junctions. The reaction produces HCl and forms a metal–oxygen bond, anchoring the complex to the surface. By using the molybdenum oxychlorides MoO_2Cl_2 and $MoOCl_4$, we would expect to form a molybdenum oxide surface and be able to investigate its properties. This would allow us to characterize the interactions of the molybdenum oxychlorides with alumina and possibly expand the range of usable surface oxides.

Molybdenum dioxodichloride and molybdenum oxotetrachloride are well suited for use in these experiments: both are monomeric in the vapor phase,[24] and both react with hydroxyl groups.[25] The oxotetrachloride reacts with water to form "molybdenum blues",[25] which are a series of mixed molybdenum(V)/molybdenum(VI) oxides. It has been suggested that the blue color is due to the formation of Mo_3 metal atom clusters.[26] Further information concerning these molybdenum blues is reviewed elsewhere.[26,27]

The two oxychlorides and the molybdenum(VI) oxide are strong Lewis acids and react readily with Lewis bases. As substantial number of $MoO_2Cl_2 \cdot 2L$ type complexes are known, where L = ether, ketone, or ester,[28] tetrahydrofuran,[29] pyridine,[30] or *N*,*N*-dimethylformamide or *N*,*N*-dimethylacetamide.[25] Each of these complexes is monomeric, in contrast to MoO_2Cl_2 in chloroform[31] or in a Nujol mull,[31] where it is dimeric or polymeric with oxygen bridges. Similarly, the molybdenum(VI) oxide is polymeric in the solid state but forms monomeric species when complexed with strong Lewis bases such as diethylenetriamine.[32] A considerable number of molybdenum oxides are known with composition intermediate between MoO_2 and MoO_3. Of these, six have been reasonably well characterized, usually by X-ray crystallography, namely Mo_4O_{11}, $Mo_{17}O_{47}$, Mo_5O_{14}, Mo_8O_{23}, Mo_9O_{26}, and $Mo_{18}O_{52}$.[33-36] These oxides are based primarily on MoO_6 octahedra, but $Mo_{17}O_{47}$ and Mo_5O_{14} are based both on MoO_6 and MoO_7 (pentagonal bipyramidal) subunits.[35,37,38] These materials exhibit a wide variation in resistivity (at 0°C), e.g., from 250 Ω·cm for $Mo_{18}O_{52}$ to 5×10^{-3} Ω·cm for $Mo_{17}O_{47}$[35-37,39] and 2.98×10^{-4} Ω·cm for MoO_2,[40,41] which is comparable to the value for bismuth (1.07×10^{-4} Ω·cm).[42] Thus, these materials have rather low resistivities and may exhibit small band gap (semiconductor) rather than large band gap (insulator) characteristics. This requires the presence of an insulator support to provide acceptable voltage characteristics for use in inelastic electron-tunneling spectroscopy. Further details and numerous references to the molybdenum suboxides are given by Manthiram and Gopalakrishnan.[43]

II. Experimental Procedures

A. Materials. The molybdenum dioxodichloride (MoO_2Cl_2, minimum purity 99%) and molybdenum oxytetrachloride ($MoOCl_4$, minimum purity 99%) were purchased from Alfa. The ethylene was Matheson CP grade (99.5% min). The acetic acid was Fischer Scientific reagent grade (assay 99.7% min). The 4-*tert*-butylpyridine was purchased from Aldrich (minimum purity 99%).

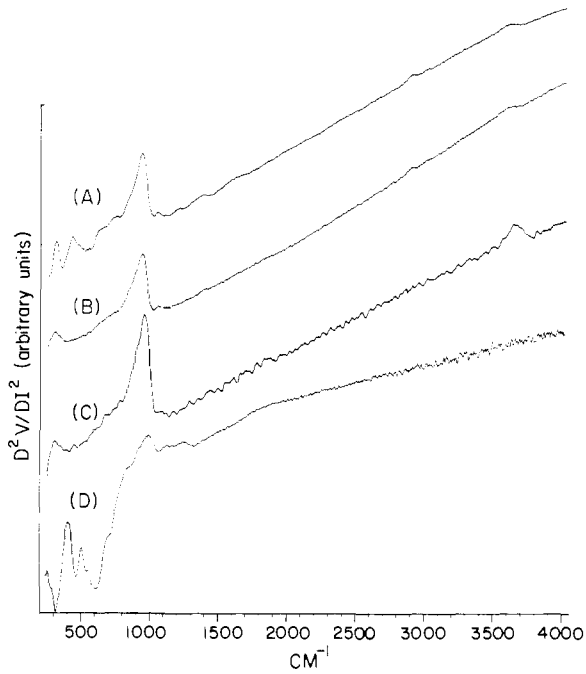

Figure 1. Tunneling spectra produced by adsorption of $MoOCl_4$ on aluminum oxide: (A) adsorption at 22 °C, (B) adsorption at 22 °C, followed by heating under vacuum to 40 °C for 900 s, (C) tunneling spectrum of a clean aluminum oxide surface (blank junction), (D) adsorption at 100 °C. Pressure of $MoOCl_4$ = 27×10^{-3} Torr, time of exposure = 300 s.

B. Junction Fabrication. The fabrication system and detailed fabrication procedures are given elsewhere.[44] Briefly, the procedure is as follows. A lower aluminum electrode, approximately 800 Å in thickness, is evaporated through a pattern-forming mask onto a glass substrate. The electrode is then annealed by heating to 100 °C for 300 s by using the method of Bowser and Weinberg.[45] This electrode is oxidized in a glow discharge (~1100 eV, 12 mA, 300 s) at a pressure of 10^{-1} Torr in a 1000:1 mixture of oxygen and water vapor. This produces an aluminum oxide film approximately 20 Å in thickness, with properties similar to those of bulk γ-alumina.[46,47] The surface of this oxide is hydroxylated due to the presence of the water vapor in the plasma discharge. The approximate hydroxyl concentration is 4×10^{14} cm^{-1},[48] and the total area of the oxidized aluminum film is approximately 0.4 cm^2.

Either molybdenum dioxodichloride or molybdenum oxytetrachloride is then adsorbed on the oxide surface from the vapor phase. Adsorption was carried out both at room temperature (22 °C) and at elevated temperatures (usually 100 °C) by resistive heating of the aluminum electrode. Some junctions were completed at this point, whereas most were subjected to further reaction. By evacuating the system to a pressure below 5×10^{-8} Torr, exposed junctions could be post-heated under vacuum.

All junctions were completed by evaporating a lead upper electrode, approximately 2500 Å in thickness, and then removed from the vacuum system and mounted on a sample holder for measurement.

C. Spectral Measurements and Data Processing. The tunneling spectra were measured with a computer-controlled data-acquisition system described in detail elsewhere.[49] The electronics consist of a constant-current modulation, second-derivative detection system operated at a junction temperature of 4.2 K in liquid helium. This second derivative (D^2I/DV^2) produces a spectrum that is analogous to an IR or Raman vibrational spectrum. The spectral data over a range between 240 and 4000 cm^{-1} were acquired with a DEC LSI 11/23 microcomputer-based system and displayed in near-real time (~10 s) on a Tektronix oscillo-

(23) Bowser, W. M.; Weinberg, W. H. *J. Am. Chem. Soc.* **1981**, *103*, 1453.
(24) Ward, B. G.; Stafford, F. E. *Inorg. Chem.* **1968**, *7*, 2569.
(25) Larson, M. L.; Moore, F. W. *Inorg. Chem.* **1966**, *5*, 801.
(26) Cotton, F. A.; Wilkinson, G. *Advanced Inorganic Chemistry*, 4th ed.; Wiley: New York, 1980.
(27) Rubin, M. B.; Day, P. *Adv. Inorg. Chem. Radiochem.* **1967**, *10*, 335.
(28) Krauss, H. L.; Huber, W. *Chem. Ber.* **1961**, *94*, 2864.
(29) Freeman, K.; Fowles, G. W. A. *Inorg. Chem.* **1965**, *4*, 310.
(30) Bernard, J.; Camelot, M. *C. R. Seances Acad. Sci., Ser. C.* **1966**, *263*, 1068.
(31) Barraclough, C. S.; Stals, J. *Aust. J. Chem.* **1966**, *19*, 741.
(32) Mazluft, W. F. *Inorg. Chem.* **1964**, *3*, 395.
(33) Magneli, A. *Acta Chem. Scand.* **1948**, *2*, 501.
(34) Magneli, A. *Acta Crystallogr.* **1953**, *6*, 495.
(35) Kihlborg L. In *Nonstoichiometric Compounds*; Ward, R., Ed.; American Chemical Society: Washington, 1963.
(36) Kihlborg, L. *Acta Chem. Scand.* **1959**, *13*, 954.
(37) Kihlborg, L. *Acta Chem. Scand.* **1960**, *14*, 1612.
(38) Kihlborg, L. *Arkv. Kemi.* **1963**, *21*, 427.
(39) Khilla, M. A.; Mikhail, H.; Abul-El-Soud, A.; Hanafi, Z. M. *Czeck. J. Phys. B* **1980**, *30*, 1039.
(40) Brandt, B. G.; Skapski, A. C. *Acta Chem. Scand.* **1967**, *21*, 661.
(41) Benadar, L.; Shimony, Y. *Mater. Res. Bull.* **1974**, *9*, 837.
(42) *Handbook of Chemistry and Physics*, 55th ed.; West, R. C., Ed.; CRC Press: Cleveland, 1974.
(43) Manthiram, A.; Gopalakrishan, J. *Rev. Inorg. Chem.* **1984**, *6*, 1.
(44) Gajda, G. J.; Weinberg, W. H. *Rev. Sci. Instrum.* **1986**, *57*, 1388.
(45) Bowser, W. M.; Weinberg, W. H. *Rev. Sci. Instrum.* **1976**, *47*, 583.
(46) Bowser, W. M.; Weinberg, W. H. *Surf. Sci.* **1977**, *64*, 377.
(47) Evans, H. E.; Bowser, W. M.; Weinberg W. H. *Appl. Surf. Sci.* **1980**, *5*, 258.
(48) Lewis, B. F.; Mosesman, M.; Weinberg, W. H. *Surf. Sci.* **1974**, *41*, 142.
(49) Gajda, G. J.; Weinberg, W. H. *Rev. Sci. Instrum.* **1985**, *56*, 700.

Table I. Vibrational Frequencies (cm^{-1}) for Molybdenum Complexes and a Formate Anion

$MoOCl_4$/IR gas phase (ref 24)	MoO_2Cl_2/IR Nujol mull (ref 31)	MoO_2Cl_2/IR diethyl ether solution (ref 31)	$HCOO^-$/alumina tunneling spectrum (ref 60)	$MoOCl_4$/alumina, tunneling spectrum Figure 1A (this work)
			2991 $\nu_s + \nu_a$ (CO_2^-)?	
			2875 ν(CH)	2900 ν(CH)
			2727 δ(CH) overtone	
			1580 $\nu_a(CO_2^-)$	1640 $\nu_a(CO_2^-)$
			1456 $\nu_s(CO_2^-)$	
			1370 δ(CH)	1375 δ(CH)
			1038 γ(CH)	1050 γ(CH)
1015 ν(Mo=O)				
		969 ν_s(Mo=O)		
			940 ν(AlO)	940 ν(AlO)
	910 ν(Mo—O)	928 ν_a(Mo=O)		
	864 ν(Mo—O)			
	827 ν(Mo—O—Mo)	830 ν(Mo—O—Mo)		
	781 ν(Mo—O—Mo)	777 ν(Mo—O—Mo)		750 ν(Mo—O—Mo)
				630 ν(Mo—O—Mo)
450 ν(MoCl)				
396 ν(MoCl)	401 ν(MoCl) + deformation modes			350- ν(MoCl) +
	376			500 δ(O—Mo—Cl)
	372	361 ν(MoCl)		
	344	358 ν(MoCl)		
	284			305 δ(O—Mo—Cl)
			242 CO_2^- rock	

scope to aid in the optimization of the phase setting of the lock-in detector. Typical data collection parameters are the following: 1.7 mV rms modulation voltage (at a bias voltage of 0.250 V), lock-in detector time constant (τ) of 3 ms, and 1000 spectral scans (of 965 points each corresponding to a 4 cm^{-1} point spacing) summed to improve the signal-to-noise ratio. The combination of thermal and modulation broadening yields an instrumental resolution of approximately 20 cm^{-1} for the operating parameters given above.

All tunneling spectra displayed in the figures are unsmoothed. Some spectra were processed further to remove the linear background slope by using a least-squares convolution algorithm to extract the average slope. Details of this method are discussed elsewhere.[50]

III. Results

A. Molybdenum Oxytetrachloride Adsorption on Alumina. Molybdenum oxytetrachloride was adsorbed on the alumina surface of the tunnel junction from the vapor phase at its (extrapolated) vapor pressure of 27×10^{-3} Torr at 22 °C.[51] Spectra of the decomposition products are shown in Figure 1, A and B. The tunneling spectrum in Figure 1A is from a junction that was at a temperature of 22 °C for 900 s after termination of the $MoOCl_4$ exposure. The tunneling spectrum in Figure 1B is from a junction that was heated to approximately 40 °C for 900 s after the termination of the $MoOCl_4$ exposure. The system pressure was below 5×10^{-8} Torr before the lead evaporation was begun. A blank junction (with no intentionally added absorbates) is shown for comparison in Figure 1C. The spectrum of Figure 1A was processed to remove the background slope and is shown in Figure 2 for the spectral region between 240 and 1100 cm^{-1}. The vibrational frequencies from the molybdenum oxytetrachloride junction are listed in Table I.

Heating the alumina surface during exposure to molybdenum oxytetrachloride vapor results in further reaction. As an example, a junction that was heated to 100 °C during exposure for 300 s is shown in Figure 1D. The majority of junctions prepared in this way with molybdenum oxytetrachloride displayed very low resistance ($R < 10\ \Omega$) or, for those with sufficient resistance to measure, extreme changes in conductivity (σ) with bias voltage. For a typical tunnel junction prepared with acetic acid, $\Delta\sigma \equiv (\sigma_{500mV} - \sigma_{30mV})/\sigma_{30mV} \sim 3$–5%. For many of the molybdenum oxytetrachloride junctions, $\Delta\sigma > 200\%$. The tunneling junction spectrum in Figure 1D had a $\Delta\sigma$ of approximately 30%. These large changes in conductance produce significant problems in a constant modulation current measurement system, such as ours, since they cause very large changes in sensitivity over the range of bias voltages. The sensitivity is proportional to the square of the modulation voltage, which in turn is equal to the fixed current divided by the conductance.

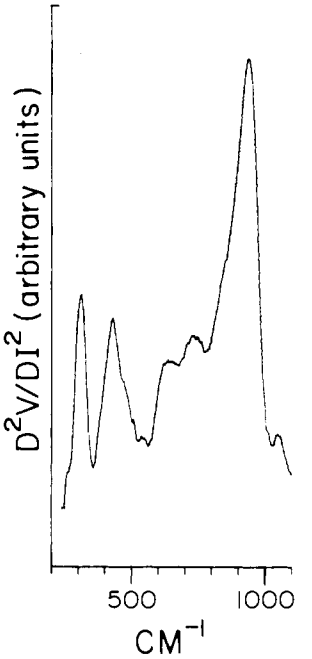

Figure 2. Tunneling spectrum from Figure 1A processed to remove the background slope. The spectral region from 240 to 1100 cm^{-1} is shown.

B. Molybdenum Dioxodichloride Adsorption on Alumina. As was the case for the molybdenum oxytetrachloride exposures, the molybdenum dioxodichloride was exposed to the alumina surface from the vapor phase at its (extrapolated) vapor pressure of 59×10^{-3} Torr at 22 °C.[52] The results of various thermal treatments are shown in Figure 3. The tunneling spectrum resulting from an exposure at room temperature for 300 s, and kept at room temperature, is shown in Figure 3A. Exposure at room temperature for 300 s, followed by heating to 100 °C for 300 s under vacuum (background pressure below 10^{-7} Torr), produces the tunneling spectrum in Figure 3B. Heating the junction to 100 °C for 300 s during the dioxodichloride exposure, followed by cooling to room temperature under vacuum, yields the tunneling spectrum in Figure 3C. Finally, the result of heating the junction to 100 °C for 300 s during the exposure, followed by heating the

(50) Gajda, G. J.; Weinberg, W. H. *J. Vaccum Sci. Technol. A* **1985**, *3*, 2208.

(51) Sacki, Y.; Matsuzaki, R. *J. Electrochem. Soc. Jpn.* **1966**, *34*, 115.

(52) Sacki, Y.; Matsuzaki, R. *J. Electrochem. Soc. Jpn.* **1966**, *34*, 180.

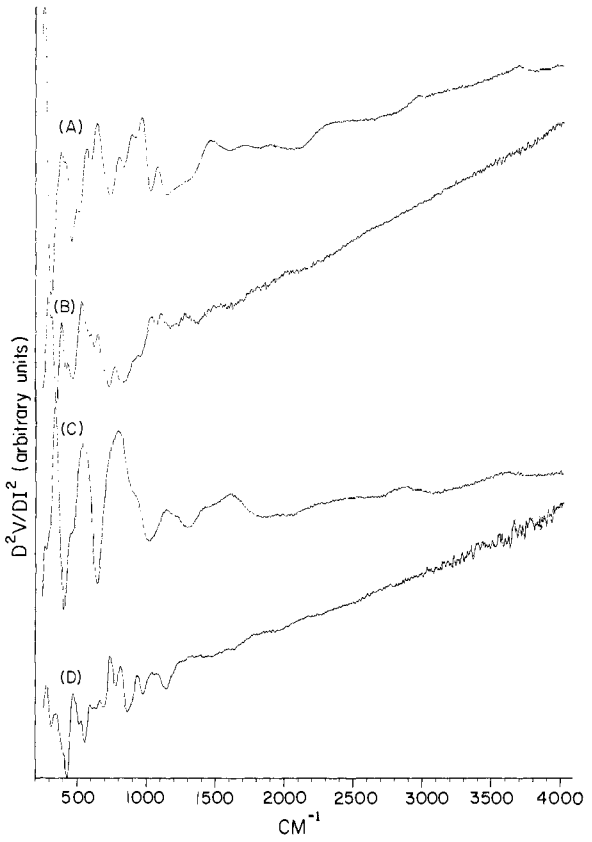

Figure 3. Tunneling spectra produced by adsorption of MoO_2Cl_2 on aluminum oxide: (A) adsorption at room temperature, no post-heating, (B) adsorption at room temperature, post-heated to 100 °C for 300 s under vacuum, (C) adsorption at 100 °C, no post-heating, (D) adsorption at 100 °C, post-heated to 100 °C for 300 s under vacuum. Pressure of $MoO_2Cl_2 = 59 \times 10^{-3}$ Torr, time of exposure = 300 s.

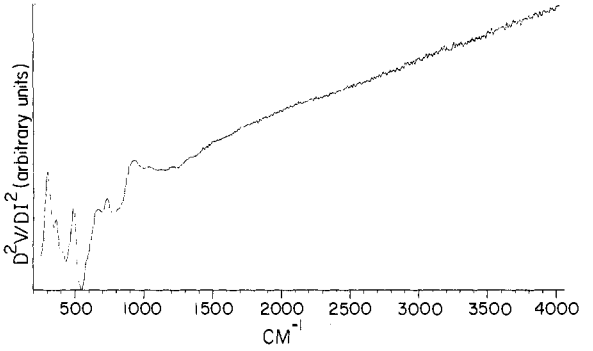

Figure 4. Tunneling spectrum of molybdenum oxide surface prepared as in Figure 3C and heated to 100 °C in 2 Torr of ethylene for 900 s.

junction to 100 °C for 300 s under vacuum, is shown in Figure 3D. Unlike the case of oxytetrachloride exposures, the majority of the junctions produced with dioxodichloride exposures exhibited only moderate ($\Delta\sigma < 50\%$) or small ($\Delta\sigma < 10\%$) conductance changes. All tunneling spectra shown are from junctions with small conductance changes.

C. Attempted Reaction of Decomposition Products of Adsorbed Molybdenum Dioxodichloride with Ethylene. The reaction product formed by heating the alumina substrate to 100 °C for 300 s during exposure to molybdenum dioxodichloride (Figure 3C) was reacted further with 2 Torr of ethylene at 100 °C for 900 s. The spectrum of the resulting product is shown in Figure 4. As discussed elsewhere,[22] the junction heating method used prevents reaching temperatures above approximately 100 °C at these pressures.

D. Reaction of Decomposition Products of Adsorbed Molybdenum Dioxodichloride with Acetic Acid and 4-*tert*-Butylpyridine. The reaction product formed by heating the alumina substrate

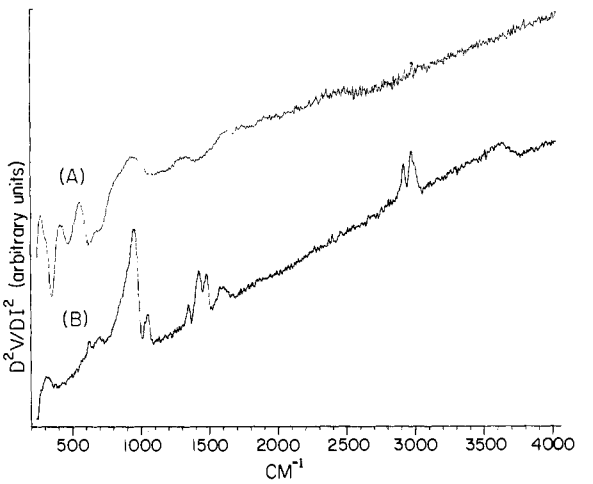

Figure 5. (A) Tunneling spectrum of molybdenum oxide surface prepared as in Figure 3C and exposed to 10^{-1} Torr of acetic acid for 300 s. (B) Tunneling spectrum of aluminum oxide surface exposed to acetic acid as in spectrum A.

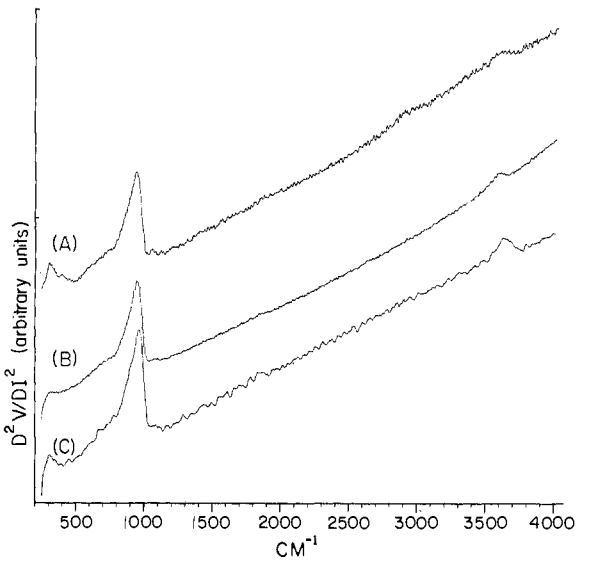

Figure 6. (A) Tunneling spectrum of molybdenum oxide surface prepared as in Figure 3C and exposed to 5×10^{-2} Torr of 4-*tert*-butylpyridine for 300 s. (C) Tunneling spectrum of a clean aluminum oxide surface (blank junction).

to 100 °C for 300 s during exposure to molybdenum dioxodichloride (Figure 3C) was reacted further with acetic acid and with 4-*tert*-butylpyridine at room temperature. The tunneling spectrum that results from an exposure to acetic acid at 10^{-1} Torr for 100 s is shown in Figure 5A, whereas the tunneling spectrum of acetic acid adsorbed on the alumina surface is shown for comparison in Figure 5B. Exposing the decomposition products of adsorbed molybdenum dioxodichloride to 4-*tert*-butylpyridine at 5×10^{-2} Torr for 100 s produced the tunneling spectrum in Figure 6A. For comparison, exposing an alumina surface to 4-*tert*-butylpyridine (10^{-1} Torr for 1000 s) resulted in the tunneling spectrum of Figure 6B, whereas the tunneling spectrum of a blank junction is shown in Figure 6C.

IV. Discussion

A. Molybdenum Oxytetrachloride Adsorption on Alumina. Exposing the alumina surface to molybdenum oxytetrachloride ($MoOCl_4$) produced the tunneling spectra in Figures 1 and 2. The vibrational frequencies listed in Table I include those of Figure 1A and Figure 2, a bidentate bridging formate on alumina due to the dissociative adsorption of formic acid, molybdenum oxytetrachloride (vapor phase), and molybdenum dioxodichloride in both a diethyl ether solution and a Nujol mull.

The tunneling spectra of $MoOCl_4$ adsorbed on alumina at 22 °C Figure 1, A and B show evidence of very slight contamination by formate (the peaks at approximately 2900, 1050, 1375, and 1640 cm^{-1}). This species results from an unintentional infusion doping of carbon dioxide in a high relative humidity atmosphere, which occasionally occurs in the laboratory, during the transfer of the completed junctions from the fabrication system to the measurement system. Under these conditions, carbon dioxide and water vapor in the atmosphere react with the lead electrode during infusion to form formic acid, which in turn reacts with the alumina to form formate and a surface hydroxyl group. Further details are discussed by Field.[53]

The major difference between the tunneling spectra in Figure 1, spectra A and B, is the presence of a strong, broad mode at 350–500 cm^{-1} (maximum at 425 cm^{-1}) and two moderately strong modes at 630 and 750 cm^{-1} which appear as shoulders on the 940-cm^{-1} aluminum–oxygen stretching mode in Figure 1A. The low-frequency modes (240–1100 cm^{-1}) in Figure 1A are shown in detail in Figure 2. The difference in intensity of the formate modes at 1375 and 1640 cm^{-1} between Figure 1, spectra A and B is due to a smaller concentration of the formate species in Figure 1B. Comparing the tunneling spectrum of Figure 1A and Figure 1B with that of an unexposed (blank) junction, Figure 1C, indicates a significant decrease in the area of the hydroxyl peak. This suggests that $MoOCl_4$ reacts with the surface to remove hydroxyl protons and forms a surface species which then desorbs slowly (cf. Figure 1B).

In Table I, the vibrational frequencies of $MoOCl_4$ adsorbed on alumina are compared with the vapor-phase infrared spectra of $MoOCl_4$ and the infrared spectrum of molybdenum dioxodichloride (MoO_2Cl_2) in Nujol (where it is polymeric) and diethyl ether (where it is dimeric).[31]

A comparison between the vapor-phase infrared spectrum of $MoOCl_4$ and the tunneling spectrum of adsorbed $MoOCl_4$ reveals significant differences between the two (e.g., the lack of a 1015-cm^{-1} ν(MO=O) in the adsorbed species). This indicates a significant structural change in the $MoOCl_4$ upon adsorption. By comparison with the infrared spectra of MoO_2Cl_2 in diethyl ether (where MoO_2Cl_2 is dioxo bridged, but not chlorine bridged) and in a Nujol mull (where MoO_2Cl_2 is tetraoxo bridged and dichlorine bridged to form a polymer), the lack of ν(Mo=O) modes at 928 and 969 cm^{-1} suggest tetraoxo bridging. Although we have no isotopic labeling data to confirm the assignments of the Mo–Cl modes, the formation of a polymolybdate species is unlikely. As discussed in Section IV.B, the reaction of MoO_2Cl_2 with the hydroxylated alumina surface does form a polymolybdate type species, *which does not desorb* when the surface is heated to 100 °C for 300 s. One possible admolecule formed is a bis(molybdenum oxochloride) complex

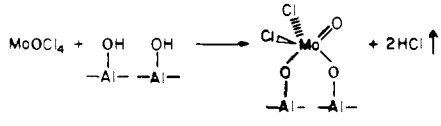

(1)

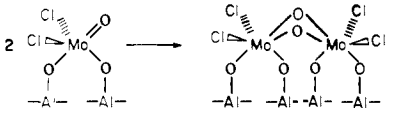

(2)

Reaction 1 is simply that of $MoOCl_4$ with the hydroxylated surface (analogous to the hydrolysis of the $MoOCl_4$), which removes the surface hydroxyl protons as HCl. Reaction 2 is the dimerization of the surface species. This species has a distored octahedral structure which is known for Mo(VI) complexes.[26] Higher nuclearity species, such as trimers, cannot be excluded.

As stated above, both spectra A and B in Figure 1 show evidence of a reduction in the surface concentration of hydroxyl groups.

(53) Field, B. O.; Hart, R.; Lewis, D. M. *Spectrochim. Acta* **1985**, *41A*, 1069.

Table II. Vibrational Frequencies (cm^{-1}) of Molybdenum Oxide Surface Complexes Formed from MoO_2Cl_2

RT/ RT[a]	RT/ 100 °C	100 °C/ RT	100 °C/ 100 °C	tentative assignment (54, 55)
3680		3680		ν(OH)
2950		2930		ν(H—O—H)
2400		2460		ν[(Mo)—O—H]
1625		1625		δ(H—O—H)
1440		1440		δ(H—O—H)
	1300		1320	δ(Mo—O—H)
		1150	1225	δ(Mo—O—H)
1090	1105		1060	δ(Mo—O—H)
	1030		1030	ν(Mo=O)
950				ν_a(O=Mo=O)
	940	940	940	ν(Al—O)
910				ν_s(O=Mo=O)
815		815	815	ν(Mo-O)
	770			ν(Mo—O)
			740	ν(Mo—O—Mo)
665	645		665	ν(Mo—O—Mo)
590	590p	590	590	ν(Mo—O—Mo)
	535		535	ν(Mo—O—Mo)
500	440	455	470	δ(Mo—O)
385	385			δ(Mo—O)
		340	345	δ(Mo—O)
260	285	270	280	δ(Mo—O)

[a] RT = room temperature.

Only Figure 1A, however, inidcates the presence of the bis(molybdenum oxochloride) complex. The lack of modes due to the bis(molybdenum oxochloride) complex in Figure 1B suggests that heating to 40 °C for 900 s has caused the complex to desorb. One possibility is for the surface complex to de-dimerize and desorb as MoO_2Cl_2, i.e.

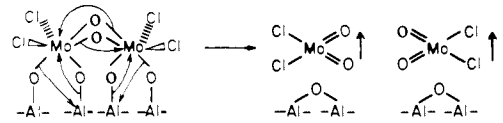

(3)

Unfortunately, the fabrication system did not have a mass spectrometer, and the composition of the desorbed molecules could not be determined.

If the alumina surface is heated during the $MoOCl_4$ exposure, tunneling spectra similar to that shown in Figure 1D are obtained. As mentioned in Section III.A, most of the junctions prepared in this manner have electrical characteristics which make them unsuitable for measuring inelastic tunneling spectra. Due to the large $\Delta\sigma$ which results in substantial background curvature, no structural or mode assignments have been attempted.

B. Molybdenum Dioxodichloride Adsorption on Alumina. The tunneling spectra that result from exposing MoO_2Cl_2 vapor to an alumina surface at either room temperature or 100 °C are shown in Figure 3, and the observed vibrational frequencies are listed in Table II. The tunneling spectra in Figure 3, A and C, were not heated after exposing the MoO_2Cl_2 to the alumina surface and show evidence of adsorbed water and molybdenum hydroxide formation, which will be discussed below. Initially, the MoO_2Cl_2 reacts with surface hydroxyl groups to form a MoO_2 (O-surface)$_2$ species with desorption of HCl. The surface species can then undergo reactions with background water vapor. Since water vapor is used during the oxidation of the aluminum electrodes, it is the major source of the background vapor pressure ($\sim 5 \times 10^{-8}$ Torr) during the pumpdown interval ($\sim$1500 s) between the end of the adsorbate exposure and the beginning of the lead evaporation.

Spectra A and B of Figure 3 exhibit modes at 1030 cm^{-1} [terminal ν(Mo=O)], 900–950 cm^{-1} [cis ν(O=Mo=O)], $\sim$600–850 cm^{-1} [ν(Mo=O=Mo)], and $\sim$300–470 cm^{-1} [δ(Mo=O)] which are characteristic of molybdenum(VI) oxides with varying degrees of oligomerization.[54,55] The oligomerized mo-

(54) Nyquist, R. A.; Kagel, R. O. *Infrared Spectra of Inorganic Compounds*; Academic: New York, 1971.

lybdenum oxide formed depends strongly on the conditions of the reaction. Characteristics of limited oligomerization are evident in the oxide formed with exposure and pumpdown at room temperature (RT/RT) (modes at 950 and 910 cm^{-1} indicate *cis*-molybdenum dioxide groups). By comparison, post-heating to 100 °C [RT/100°C, Fig. 3(B)] reveals a loss of intensity near 900 cm^{-1} (the 940-cm^{-1} shoulder is due to the aluminum oxide stretch), and an increase in intensity in the 500–700-cm^{-1} region (indicating bridging oxygen modes) and at 1030 cm^{-1} (probably the terminal molybdenum–oxygen double bond stretch[55]).

Similarly, the 100 °C exposure without post-heating (100 °C/RT, Figure 3C) produces no modes characteristic of *cis*-molybdenum dioxo species yet has broad modes centered at 590 and 815 cm^{-1}, indicating oligomerized molybdenum oxide species (in this case, also with chemisorbed water). Finally, the post-heated junction (100 °C/100 °C, Figure 3D) gives spectra related both to the RT/100 °C and 100 °C/RT spectra. The extent of oligomerization is quite high[54,55] as evidenced by the lack of modes near 900–950 cm^{-1}. The terminal molybdenum–oxygen double bond at 1030 cm^{-1} is partially obscured due to the broadness of the δ(Mo–O–H) mode at 1060 cm^{-1}. As in the room temperature post-heated spectrum, there is little evidence of adsorbed water, although the modes at ~1100 and ~1300 cm^{-1} suggest the presence of residual molybdenum hydroxide species. The ν(OH) mode for the hydroxyl groups is too broad to be observed.

Nyquist and Kagel[54] discuss the vibrational modes observed in inorganic compounds due to water of hydration and metal hydroxide (formed by the interaction of water and the metal oxide). They assign modes of ν(OH) at 2800–3400 cm^{-1} and δ(H–O–H) at 1590–1660 cm^{-1} as due to the water of hydration (analogous to chemisorbed water on the oxide surface) and ν(OH) at 2000–3200 cm^{-1} and δ(M–O–H) at 950–1200 cm^{-1} as due to metal hydroxide formation. The infrared spectrum of hydrated MoO_3[54] shows modes at 1150, 1350, 1630, 2300, and 3200–3700 cm^{-1}. By comparison, an infrared spectrum of rigorously dried MoO_3 shows no vibrational modes between 1000 and 4000 cm^{-1}.[56] The disappearance of the 2930–2950-[ν(HOH)] and 1625-cm^{-1} [δ(HOH)] modes in the tunneling spectrum upon post-heating the tunneling junctions (100 °C for 300 s at 1×10^{-7} Torr) strongly suggests the interaction of water vapor with the molybdenum oxide that is formed by the hydrolysis of the MoO_2Cl_2 by the surface hydroxyl groups.

The stability of coordinated molecular water in molybdenum complexes is well-established. The "hydrates" of MoO_3, $MoO_3 \cdot H_2O$ and $MoO_3 \cdot 2H_2O$, are actually $MoO_2(OH)_2$ and $MoO_2(OH)_2 \cdot H_2O$, respectively. Thermal desorption studies by Sotani et al.[57] show desorption maxima of water at 150 and 400 °C for desorption at 10^{-3} Torr. These peaks are attributed to desorption of coordinated water and the recombination of hydroxyl groups, respectively. A transmission infrared study of water chemisorbed on MoO_3 by Chung et al.[58] verifies the existence of molecularly chemisorbed water by the presence of the H_2O scissoring mode at approximately 1650 cm^{-1}. The water chemisorbs at coordinatively unsaturated molybdenum sites.[58]

These oxide surfaces, unlike those formed by the $MoOCl_4$, produce tunnel junctions with reasonably useful electrical characteristics ($\Delta\sigma \sim$ 5–10%). Some preliminary experiments to investigate the surface properties of these molybdenum oxides are discussed below.

C. Attempted Reaction of the Decomposition of MoO_2Cl_2 Adsorbed on Alumina at 100 °C with Ethylene. As discussed elsewhere,[22] we have attempted to react a molybdenum oxide surface species, formed by the decomposition of molybdenum hexacarbonyl, with ethylene in order to form an oxomolybdenum carbene species of the type proposed as the active catalyst for metathesis reactions. A discussion of the metathesis reaction and the proposed mechanism is given in the review by Grubbs.[59]

Similarly, we attempted to activate with ethylene the oligomerized molybdenum oxide surface produced by surface hydrolysis of MoO_2Cl_2 with ethylene (Figure 3C). The tunneling spectrum that resulted from a 2-Torr exposure of ethylene at 100 °C for 900 s is shown in Figure 4. Heating times of up to 1800 s were used with essentially the same result: no evidence of carbene formation. The exposure of the molybdenum oxide surface to ethylene at 100 °C has resulted in the desorption of the chemisorbed water (due to the post-heating) as well as most of the hydroxyl groups [indicated by the weak δ(Mo–O–H) modes] at longer heating time. The oxide is also extensively oligomerized as indicated by the weak ν(Mo=O) mode at ~1030 cm^{-1}. These changes are caused by the longer annealing time.

D. Reaction of the Molybdenum Oxide Surface Formed by Decomposition of MoO_2Cl_2 on Alumina at 100 °C with Acetic Acid and 4-*tert*-Butylpyridine. The tunneling spectra that result from the hydrolysis of MoO_2Cl_2 display evidence of water chemisorbed on the molybdenum oxide surface. This indicates that the coordinatively unsaturated molybdenum oxide is functioning as a Lewis acid (at the molybdenum center) by coordinating the Lewis base, water. This is in contrast to the coordinatively saturated hydroxylated alumina surface, which shows no evidence of coordinated water under normal preparation conditions. The aluminum oxide junctions react with Brønsted acids, such as acetic acid, to form the corresponding conjugate base of the acid (e.g., acetate) and water, which desorbs under vacuum, or an additional surface hydroxyl group. By contrast, Lewis bases such as 4-*tert*-butylpyridine are weakly chemisorbed and readily desorb under vacuum. We thus undertook a preliminary study of the acid/base behavior of the molybdenum surface.

The molybdenum oxide surface that is formed, as noted above, is relatively sensitive to the preparation conditions. Thus all experiments were controlled with the temperatures of exposure maintained at 100 ± 5 °C and the times of exposure 300 ± 1 s. The temperature in the laboratory was stable to ±0.2 °C (at 22.0 °C) during the experimental series. This corresponds to a $\pm 1 \times 10^{-3}$ Torr change in the vapor pressure or an error in the exposure of ±2%. Thus the initial molybdenum oxide surface corresponds to the tunneling spectrum in Figure 3C.

The result of an exposure of acetic acid vapor at 10^{-1} Torr for 300 s is shown in the tunneling spectrum of Figure 5A. For comparison, the result of an identical exposure of acetic acid on an alumina surface is shown in Figure 5B. The differences are substantial. There are no sharp peaks characteristic of acetate formation on the molybdenum oxide surface. However, the absence of the ν(OH) mode at 3650 cm^{-1}, even though the oxide was not heated, as well as several peaks between 1200 and 3000 cm^{-1} indicate decomposition of the acetic acid. The broad, weak modes produced by the decomposed acetic acid do not allow identification of the decomposition product.

By contrast, the tunneling spectrum that results from an exposure of 4-*tert*-butylpyridine vapor at 5×10^{-2} Torr for 100 s on the molybdenum oxide surface is shown in Figure 6A. For comparison, the tunneling spectrum from a junction exposed to 10^{-1} Torr of 4-*tert*-butylpyridine vapor for 100 s on an aluminum oxide surface is shown in Figure 6B, and the tunneling spectrum of a blank junction is shown in Figure 6C. It is immediately obvious that all modes characteristic of molybdenum oxide are missing in Figure 6A, as well as the vibrational modes due to a large fraction (~50–60%) of the surface hydroxyl groups. Exposure of an alumina surface to 200 times as much 4-*tert*-butylpyridine produces a tunneling spectrum, Figure 6B, similar to that of a blank junction, Figure 6C. The relative surface hydroxyl coverage is determined by comparing the ratio of the area of the ν(OH) peak normalized to the area of the ν(Al–O) mode for the sample spectrum to the corresponding ratio for a blank junction. The MoO_2Cl_2 exposure, followed by 4-*tert*-butylpyridine exposure,

(55) Buckley, R. I.; Clark, R. J. H. *Coord. Chem. Rev.* **1985**, *65*, 167.
(56) See, for example, Sadtler Infrared Spectrum Y924K.
(57) Sotani, N.; Masuda, S.; Kishimoto, S.; Hasegawa, M. *J. Colloid Interface Sci.* **1979**, *70*, 595.
(58) Chung, J. S.; Miranda, R.; Bennett, C. O. *J. Chem. Soc., Faraday Trans. 1* **1985**, *81*, 19.
(59) Grubbs, R. H. In *Comprehensive Organometallic Chemistry*; Wilkinson, G.; Ed.; Academic: New York, 1985; Vol. 8, pp 499–551.
(60) Walmsley, D. G.; Nelson, W. J.; Brown, N. M. D.; Floyd, R. B. *Appl. Surf. Sci.* **1980**, *5*, 107.

produces a decrease in the surface hydroxyl coverage of ~50–60%, whereas the 4-*tert*-butylpyridine exposure alone produces a decrease of ~15–20%. This suggests that, in fact, the MoO_2Cl_2 reacted with the surface hydroxyl groups to form the molybdenum oxide surface and desorb the hydroxyl protons as HCl. The 4-*tert*-butylpyridine then reacted with the oligomerized molybdenum oxide and desorbed the molybdenum oxide from the surface.

Nitrogen-containing bases (e.g., diethylenetriamine) are sufficiently strong to produce depolymerization of molybdenum oxide.[32] This suggests the reaction sequence

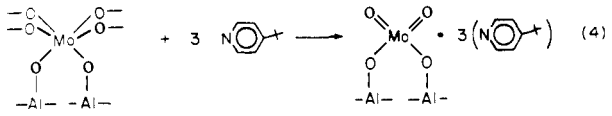

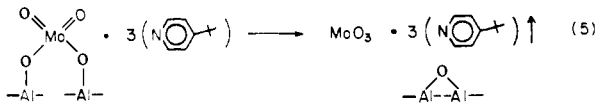

The ratio of three molecules of 4-*tert*-butylpyridine to one molecule of MoO_3 is hypothetical, but it is based on the observed octahedral coordination of MoO_3 with three basic sites for ligands. There is more than sufficient 4-*tert*-butylpyridine present in the system to satisfy the proposed stoichiometry.

The extremely strong reaction of the molybdenum oxide with Lewis bases suggests that further investigations with weaker bases or much lower exposures may produce data complementing the primarily Brønsted acid nature of adsorbates on hydroxylated aluminum oxide. In addition, molybdenum oxide is used widely as a catalyst for oxidation reactions either by itself or in the form of a mixed oxide.[21] The availability of relatively volatile (e.g., vapor pressure $>10^{-2}$ Torr) halogen or other salts of many metals suggests the possibility of generalizing this method of oxide generation to other metal systems and the formation of mixed metal oxide surfaces. Finally, the availability of dehydroxylated alumina surfaces provides the opportunity for comparison with the hydroxylated alumina surfaces used heretofore in tunneling spectroscopy.

V. Conclusions

The reaction of $MoOCl_4$ with the hydroxylated alumina surface produces a probable dimeric, oxygen-bridged surface species analogous to dimeric MoO_2Cl_2. This species is unstable with respect to desorption under vacuum. Heating the surface during exposure to $MoOCl_4$ produces a molybdenum oxide surface that is poorly suited to tunneling spectroscopy.

Reacting MoO_2Cl_2 with the hydroxylated alumina surface produces a series of molybdenum oxide surface species. The degree of oligomerization depends on the extent of heating. Surface species which have not been post-heated under vacuum give spectral evidence for adsorbed water and molybdenum hydroxide formation. Post-heating removes the chemisorbed water.

The molybdenum oxide surface displays little reactivity toward ethylene exposed at 100 °C. The molybdenum oxide surface causes decomposition of acetic acid adsorbed at 22 °C. The oxide reacts with 4-*tert*-butylpyridine, present in substantial excess, causing desorption of the molybdenum oxide, possibly as a volatile $MoO_3 \cdot 3$(pyridine) complex. The resulting surface is dehydroxylated aluminum oxide.

The use of volatile metal oxochlorides to form suitable metal oxide surfaces for study by tunneling spectroscopy has been established. Future work on molybdenum and other metal oxide surfaces formed by halide hydrolysis, as well as the availability of dehydroxylated alumina surfaces, has the potential to expand significantly the variety of surfaces capable of being studied by inelastic electron-tunneling spectroscopy.

Acknowledgment. This research was supported by the National Science Foundation under Grant No. DMR-8500789.

Rotational Spectra and Structures of the Small Clusters Ar_3–HF and Ar_3–DF

H. S. Gutowsky,* T. D. Klots, Carl Chuang, John D. Keen, C. A. Schmuttenmaer, and Tryggvi Emilsson

Contribution from the Noyes Chemical Laboratory, University of Illinois, Urbana, Illinois 61801. *Received February 13, 1987*

Abstract: Microwave rotational spectra have been observed for the two small clusters $^{40}Ar_3$–HF and $^{40}Ar_3$–DF, the first clusters to be so characterized. Their detection was made possible by sensitivity improvements to a Flygare spectrometer, which uses Fourier transform operation of a Fabry–Perot microwave cavity in conjunction with a pulsed supersonic nozzle to generate the clusters. The symmetric top transitions measured for $J = 1 \rightarrow 2$ to $J = 6 \rightarrow 7$ are fitted by rotational constants B_0, D_J, and D_{JK} of 1188.212 MHz, 6.85 kHz, and −5.76 kHz for Ar_3–HF and of 1180.379 MHz, 6.57 kHz, and −5.156 kHz for Ar_3-DF. The composition and C_{3v} symmetry of the clusters were established by the conditions of their formation, by the hyperfine structure of their transitions, by the absence of K states other than 0, ±3, and ±6, and by analysis of the values found for B_0. The H/DF lies along the threefold axis of the Ar_3 group, with the H/D end closest to Ar_3. Analysis of the moments of inertia and torsional amplitudes for the two isotopic species gives an approximate Ar_3 c.m. to HF c.m. distance of 2.735 Å and an estimate of 3.835 Å for the Ar–Ar distance. Tilt of the Ar_3 group is considered in the estimate. The Ar to HF c.m. and Ar–Ar distances in the clusters are comparable with those in the Ar_2 and Ar–HF dimers and Ar_2-HF trimer. The shape of the interaction potential between Ar_3 and the H/DF is discussed.

During the past 15 years pure rotational spectra have been studied for the ground vibrational state of a considerable number and variety of dimers formed by hydrogen bonding or van der Waals forces.[1] The more strongly hydrogen-bonded species have been investigated by Stark-modulation microwave spectroscopy of cooled gas mixtures at equilibrium.[1] Two experimental approaches have been employed for the more weakly bonded species, both previously limited to the study of dimers[2]—the molecular beam electric resonance method of the Klemperer group,[3] and

(1) Legon, A. C.; Millen, D. J. *Chem. Rev.* **1986**, *86*, 635.

(2) See, for example, Leopold, K. R. (Ph.D. Thesis, Harvard University, 1983), who describes an inconclusive search for Ar_2-OCS.

(3) Bowen, K. H., Jr. Ph.D. Thesis, Harvard University, 1977. Dyke, T. R.; Tomasevich, G. R.; Klemperer, W. *J. Chem. Phys.* **1972**, *57*, 2277.

0002-7863/87/1509-5633$01.50/0